Robotica (2013) © Cambridge University Press 2013
doi:10.1017/xxxx

Learning and Reproduction of Therapists Semi-Periodic Motions during Robotic Rehabilitation

Carlos Martinez*, Mahdi Tavakoli

Department of Electrical and Computer Engineering, University of Alberta, Edmonton, Alberta, Canada

(Accepted AUGUST 8, 2018.)

SUMMARY
The demand for rehabilitation services has increased in recent years due to population aging. Due to the limitations of therapists time and healthcare resources, robot-assisted rehabilitation is becoming an appealing, powerful and economical solution. In this paper, we propose a solution that combines Learning from Demonstration (LfD) and robotic rehabilitation to save the therapists time and reduce the therapy costs when the therapy involves periodic or semi-periodic motions. We begin by modeling the therapists behavior (a periodic or semi-periodic motion) using a Fourier Series (FS). Later, when the therapist is no longer involved, the system reproduces the learned behavior modeled by the FS using a robot. A second goal is to combine the above with Gaussian Mixture Model (GMM) and Gaussian Mixture Regression (GMR) to obtain a more flexible and generalizable reproduction of the therapists behavior. This algorithm allows learning and imitating repetitive movement tasks. Our experimental results show the application of these algorithms to repetitive motion task.

KEYWORDS: Learning from demonstration; robotic rehabilitation; Fourier series.

1. Introduction

Machine learning is a field of math and computer science that uses statistical and probability techniques to provide computer systems the ability to automatically learn from experience without explicit programming. Due to its robustness, it is widely use to make predictions of an event based on input data. Machine learning has become one of the most powerful and popular tools in the last years. It has been implemented in different fields such as civil engineering, mining, oil industry, hardware industry, finances, and computer sciences among others. The robotics field is probably one of the most affected fields due to the fast growth and innovation introduced by machine learning. Robots can be found almost in every field, from industrial automation to space exploration to medical applications. In this paper, we will be focusing on the medical application of robots especially in the post-disability physical rehabilitation and assistive technologies field. Due to the motor-sensory problems presented after a disabling event, the combination of machine learning and medical robotics could bring a huge impact to the rehabilitation scene as described in the following.

An example of physically disabling events is stroke, which has become one of the most common causes of movement disorders worldwide.[1,2] Symptoms associated with stroke often include loss of motor control, leading to difficulties in performing voluntary movements in upper and lower limbs.[3] As a consequence, people with disability are usually not able to perform activities of daily living (ADL), which are basic daily self-

* Corresponding author. E-mail: martnez@ualberta.ca

care activities such as grooming, bathing, etc.[4] To regain strength and mobility, the brain should rewire neurological pathways through therapy exercises that engage patients in repetitive tasks.[5] Traditionally, a physical therapist interacts with the patient to guide the patient through different tasks throughout the therapy. To do so and to complete a given task, the therapist usually holds the patients affected limb. This technique is called hand-over-hand therapy and is widely used to guide the patient through the task and to get feedback about the patients abilities.[6–8] Based on the obtained feedback, the therapist can decide either to assist the patient to complete the task or resist against the patients motion to make the task more challenging; this is known as assistive or resistive therapy, respectively.[9,10] The task and the intensity, length, and complexity of the therapy are chosen by the therapist depending on the patients needs. A common target for post-stroke therapy is to regain the ability to perform ADLs. ADLs are widely used because the level of patients success in such activities is a metric for the effectiveness of the rehabilitation process.[11] Due to the increasing number of people with disability, the demand for therapeutic services has also increased. Therapists and therapy resources are limited and cannot answer all requests for therapeutic services. Also, hand-over-hand movement therapy is physically exhausting for therapists when the task is repetitive. To respond to this increasing burden on the healthcare system, robotics-assisted rehabilitation has emerged as an efficient and cost-effective solution. With robot-assisted therapy, the duration and number of training sessions can be increased while reducing the workload of therapists. Rehabilitation robots are generally pre-programmed to execute a predefined task.[12] This approach does not take advantage of the robots abilities to adapt to different situations and patients. Robots reprogramming by demonstration allows adjustment of the parameters of therapy on the fly. Since these adjustments are made by therapists based on the patients needs and motion tolerances, the rehabilitation therapy is made more personalized and natural. If the robot can learn the required task-specific assistance from the therapist, only a short interaction between the therapist and the patient is sufficient. Then, in the therapists absence, the robot autonomously assists the patient similar to the therapist when performing the same task. The initial short interaction between the therapist and the patient is beneficial as it leverages the therapists experience and allows to combine the therapists skills and experience with robotic therapy. As mentioned before, therapists have the knowledge and skill to determine the required assistance or resistance for a given patient in a given phase of recovery and are also able to modify or adapt the given task based on patients necessities. Because robots do not have this ability, a therapist has to be involved at least for a short duration at the beginning of rehabilitation therapy. In this paper, we propose to use LfD as a solution to reprogram rehabilitation robots based on observing a brief window of therapist-patient interaction. The proposed LfD algorithm allows the robot to be reprogramed as a therapist moves the robot while it is in a passive (compliant) mode; this teaching method is known as kinesthetic teaching.[13] This step is known as the learning or demonstration phase. Later, when the therapist is no longer with the patient, the robot reproduces the learned therapists behavior; this step is known as the reproduction phase. In kinesthetic teaching, the therapists do not need to have any knowledge about robot programming. The main goal of the proposed system is to learn the periodicity of a repetitive task by using parameters such as amplitude and frequency. The system doesnt learn a trajectory based on position values, it learns a periodic motion based on frequencies and amplitudes. This way allows to learn more complex trajectories with less data. The paper is divided as follows: first, we explain the related works in Section 2. A description of the task is presented in Section 3. Section 4 describes the LfD algorithms to be used. Experiments are presented in Section 5. Section 6 presents the obtained results. Finally, conclusions and future work are presented in Section 7.

2. Related work

As mentioned before, ADLs are widely used in rehabilitation as a basis to design training strategies to regain strength and mobility.[14] Rehabilitation task can be divided into reaching tasks or functional tasks. Regardless of this categorization, the motions involved in a task can be either non-repetitive or repetitive. As described next, most of the past research has focused on learning and imitation of the non-periodic trajectories. As mentioned in,[15–17] previously developed algorithms can be used for learning reaching motion tasks. Given that some of the most common ADLs involve repetitive motions, it could be hard to learn and reproduce them using the current algorithms. Our goal is to extend the current LfD techniques to learn not only reaching motions but also repetitive motions, allowing therapists to use rehab robots in more diverse ADL tasks. This ability should bring benefits regarding the recovery time and the quality of the therapy. Our research group has developed robotic rehabilitation schemes that try to improve therapies through the incorporation of LfD. In,[18] the author proposed the use of LfD to realize direct bilateral telerehabilitation that encompasses two distinct phases to achieve time-sharing of a therapist. In the first phase, the system learns the therapists impedance. Later, in the second phase, the system uses the learned impedance to reproduce the therapist behavior in his/her absence. In,[19] a telerobotic cooperative rehabilitation system based on GMM and GMR is used for learning and imitation phases, respectively. In the learning phase, the therapist interacts with the patient in a cooperative task. Later, in the demonstration phase, the system learns the therapists position-based behavior and replicates it in his/her absence when the patient is alone interacting with the robotic system. In,[7] the authors developed a robot-assisted rehabilitation system for co-operative therapy combining LfD and Assist-as-Needed. In the demonstration phase, the system learns the therapists impedance using GMM. Later, GMR is used to build a model of the therapists behavior. Based on the difference between the patients performance and the learned therapists behavior, the method determines whether to assist the patient completing the task or not. As can be seen in the previous works, LfD has been used for position, force, and impedance tasks, but there is a lack of implementation of LfD into periodic motion tasks. Due to the importance of periodic motion tasks in the rehabilitation field, we decided to implement and develop the proposed system to improve the availability of rehabilitation tasks. One of the most important limitations of the previously presented work is the fact that they can only be used to learn reaching tasks. However, as mentioned before, ADLs are not limited to reaching motions. In this paper, we have a special interest in periodic motion tasks such as brushing the teeth, combing the hair, cleaning a surface with a wipe, cutting vegetables, amongst others. These periodic motion tasks are essential due to their impact in our daily life. The lack of an ability to learn repetitive motion tasks constraints the capabilities of the LfD-based robotic systems in the rehabilitation field. While it is theoretically possible to segment a semi-periodic motion trajectory into small pieces, where each piece represents a reaching motion, this learning approach has limitations. The most important limitation is the fact that it does not leverage or learn the periodicity information. Thus, an improvement is needed for a robot to learn repetitive tasks. The contributions of this paper are to use, implement and combine LfD algorithms to be able to learn repetitive motion tasks using Fast Fourier Transform (FFT) and Fourier Series (FS) as well as Gaussian Mixture Model (GMM) and Gaussian Mixture Regression (GMR). While the GMM/GMR based algorithms were created to learn how to reach a target in the spatial domain, our system tries to learn how to reach a frequency and amplitude in the frequency domain.

3. Task Description

While the proposed framework is task-independent in the sense that the system can learn and reproduce any given repetitive behavior, two representative tasks are considered here. For the first task, we have a 1-DOF (degree of freedom) motion while for the second task we have a 2-DoF motion. In the first task, the goal is to move the robots end effector

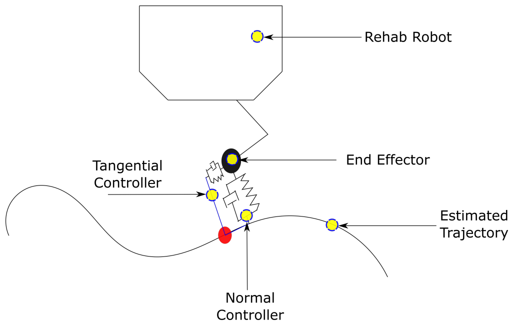

Fig. 1. First, during the demonstration phase, the therapist performs the task for a short time. Then, using robot learning from demonstration, the task is modelled as an average trajectory and variations in trajectory. The controller assists the patient by two varying impedance models (spring-damper) to follow the demonstrated trajectory and remain in the demonstrated range of variability.

in a repetitive way between two points. The robot must learn to perform the repetitive task following the demonstrated frequency and with the demonstrated amplitude. In the second task, the goal is to move the robots end effector along a 2D path in a repetitive way. The robot must learn to perform the repetitive task following the demonstrated frequency and on the demonstrated path. The next section proposes two different learning methods. The first method relies on FS while the second method combines FS, GMM, and GMR. These two methods and the two tasks mentioned above create four possible combinations (or scenarios), three of which are implemented in this paper. The first scenario combines the first method and the first task. The second scenario combines the first method and the second task. The third scenario combines the second task and the second method. The task has to be divided into two phases. In the learning phase, the therapist moves the robot to execute the task for a short duration. The robotic system uses position sensors to record the therapists trajectory. Based on the recorded data, the system builds a model of the demonstrated behavior. Later, in the reproduction phase, when the therapist is no longer interacting with the robot, the robotic system reproduces the demonstrated trajectory. Due to the presence of a patient in the reproduction phase, the robotic system will measure the patients behavior, compare it with the demonstrated behavior, and only compensate for the difference between the behavior demonstrated by the therapist and that shown by the patient. 1 shows a diagram of the task. Details related to this controller are presented in Section IV.

4. Proposed Framework

One solution to the high demand for therapeutic services is to learn the therapists behavior and replicate it for the patient later when the therapist is unavailable. Given the nature of the proposed task, Fourier Series (FS) is considered as an easy and accurate way to model the therapists behavior. Using FS, the therapists semi-periodic motion can be modeled as a sum of sinusoidal and cosines signals, where each signal has a particular frequency and amplitude. In the first and second scenarios, the main idea is to determine the frequencies and amplitudes of the FS terms. Based on the obtained results, the system models and learns the therapists behavior in the demonstration phase. Later, during the reproduction phase, the system compares the patients performance against the therapists demonstrated behavior, and by using a position controller, the robotic system reduces the difference between the patient and therapists performance. The third scenario involves the combination of GMM, GMR, and FS. As in the previous scenarios, FS is used to model the therapists behavior. The novelty, compare to the previously implemented methods emerges in the combination of GMM and GMR. In this section, we explain the demonstration and reproduction phases with detail.

4.1. First Scenario

4.1.1. Demonstration Phase. Using an FS[20] and based on the simple repetitive task described in Section III, the therapists motion is modeled as

$$f(t) = a_0 + \sum_{n=1}^{N} a_n \cos(n\omega t) + b_n \sin(n\omega t) \tag{1}$$

$$a_0 = \frac{1}{M}\,\mathrm{Re}\,(F_0) \tag{2}$$

$$a_n = \frac{2}{M}\,\mathrm{Re}\,(F_n) \tag{3}$$

$$b_n = \frac{2}{M}\,\mathrm{Im}\,(F_n) \tag{4}$$

where a_0 is a constant term, is the fundamental frequency of the signal, N is the number of harmonics in the series, t is the time, M the number of data points in the signal $f(t)$, F is the n^{th} Discrete Fourier Transform (DFT) of $f(t)$, and T is the period of the signal. Notice that $\Delta = \{a_0, a_n, b_n\}$ are unknown parameters called Fourier Series Coefficients (FSC). In order to find these parameters, (1) is used in combination with (2), (3), and (4). Once we estimate the Δ parameters, the FS given by (1) is used as a generalization of the therapists behavior. This newly learned behavior is used in the reproduction phase to help the patient to complete the given task.

4.1.2. Reproduction Phase. During the reproduction phase, the system measures the patients performance and compares it versus the behavior previously demonstrated by the therapist and modeled in (1). The difference between the two behaviors is used as the input to the robot position controller. The position controller takes the error and keeps the patients behavior as close as possible to the therapists demonstrated behavior. The controller assists the patient by two varying impedance models (spring-damper) to follow the average demonstrated trajectory and remain in the range of variability of the demonstrated trajectories. One spring-damper system assists the patient along the tangent to the trajectory, while the second spring-damper system assists the patient along the normal to the trajectory. The controller along the normal gives the patient the freedom to move within a small range of motion close to the estimated position, while the controller along the tangent assist the patient in following the right position and frequency. This controller assist the patient to reproduce the desired trajectory but it also allows the patient to have some freedom, in this way, the patient is not forced to follow exactly the same frequency and amplitude. These type of controller has been used before for trajectories, but trajectories involving periodic motions by following a frequency and amplitude are a new field for these controllers. To implement these controllers, tangential and normal lines to the estimated trajectory have to be found for every given point. The tangent can be found through the slope m between two consecutive points. Once we have the slope of the tangent, we have to compute the angle between the fixed frame and the dynamic. Finally, the current robots end effector position has to be transformed from the fixed to the dynamic frame. Once the robots position is represented in the dynamic frame, we can use a simple PD controller along each axis of the new frame. In this way, a spring-damper system can control the robot along the tangent and normal lines. The previous transformations can be executed inside the controller block of the block diagrams of 2 and 4. Notice that this frame changes for every new estimated point. Therefore, this computation runs through the whole therapy time. 2 illustrates a diagram of the fixed and the dynamic frames.

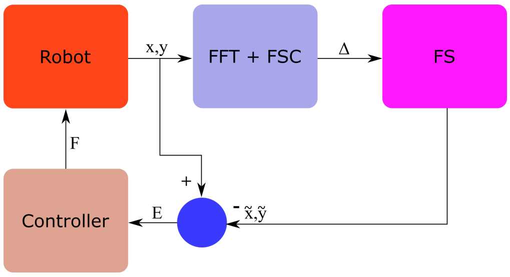

Fig. 2. Block diagram of the system used for Scenarios 1 and 2.

4.2. Second Scenario

4.2.1. Demonstration Phase. As mentioned in Section III, the second task involves a 2D periodic motion. The 2D motion can be decomposed into two 1D motions. The idea is to use the same approach as in the first scenario for X-axis and Y-axis independently.

4.2.2. Reproduction Phase. The reproduction phase is similar to the one used for Scenario 1. Because Scenario 2 has 2D, the reproduction has to be implemented for each axis. The system controls X-axis and Y-axis independently. Notice that any D-dimensional periodic movement can be easily learned, generalized and reproduced using this algorithm. The fact that the 1D task can be scaled to any dimension shows the power of this algorithm. 2 shows a block diagram for the reproduction phase used in scenarios 1 and 2. In this figure, x, y represent the current robots end effector position, $\tilde{x}, \tilde{y}$ represent the estimated position during the reproduction phase, E represents the error between the current position and the estimated position, and F represents the force needed to move the robot to the estimated position.

4.3. Third Scenario

GMM and GMR are widely used in LfD due to their robustness and well-defined implementation. The way they work can be explained as follows: The GMM algorithm takes N demonstrations of p data points. The algorithm clusters the data points in K different Gaussians, where each Gaussian has its own mean and covariance matrix. A mixture of Gaussians is later used to combine the previously computed Gaussians. This is used by the GMR to reconstruct the output. The GMR algorithm uses the previously computed GMM data and, based on the inputs; it retrieves an estimation of the expected output.[21] We implement the GMM and GMR algorithms using the code presented in.[22]

4.3.1. Demonstration Phase. During the demonstration phase, the GMM algorithm is used to build a model based on the therapists behavior. The GMM is a weighted sum of K component Gaussian densities, and it is given by the equation,

$$p(\xi_j) = \sum_{k=1}^{K} p(k) p(\xi_j|k) \tag{5}$$

where $p(k)$ is priors, $p(\xi_j|k)$ is the conditional density function and ξ_j is a D-dimensional continuous-valued dataset vector defined by $\{\xi_j\}_{j=1}^{N} = \{\xi_{p,j}, \xi_{\Delta,j}\}_{j=1}^{N}$. The dataset consists of N data points of a 2D component in polar coordinates $(\xi_{p,j})$, and a 3D component with the Δ values $(\xi_{\Delta,j})$. The variables in (5) are defined as

$$p(k) = \pi_k \tag{6}$$

$$p(\xi_j|k) = \mathcal{N}(\xi_j; \mu_k, \Sigma_k) = \frac{1}{\sqrt{(2\pi)^D |\Sigma_k|}} e^{-\frac{1}{2}\left((\xi_j-\mu_k)^T \Sigma_k^{-1} (\xi_j-\mu_k)\right)} \tag{7}$$

Thus, each Gaussian component is described by the parameters $\{\pi_k, \mu_k, \Sigma_k\}_{k=1}^{K}$, representing prior probabilities, mean vectors and covariance matrices, respectively. To get the maximum-likelihood estimation of the mixture parameters, the Expectation-Maximization (EM) algorithm has been widely used in the literature.[23] By starting from a rough estimation of the Ω parameters by k-means segmentation, it takes the GMM parameters and iterates them until convergence is reached. To guarantee an increase of the likelihood, this algorithm uses a simple local search technique. The equations for the EM algorithm are given by the following. E-step:

$$p_{k,j}^{(t+1)} = \frac{\pi_k^{(t)} \mathcal{N}\left(\xi_j; \mu_k^{(t)}, \Sigma_k^{(t)}\right)}{\sum_{i=1}^{K} \pi_i^{(t)} \mathcal{N}\left(\xi_j; \mu_i(t), \Sigma_i^{(t)}\right)} \tag{8}$$

$$E_k^{(t+1)} = \sum_{j=1}^{N} p_{k,j}^{(t+1)} \tag{9}$$

M-step:

$$\pi_k^{(t+1)} = \frac{E_k^{(t+1)}}{N} \tag{10}$$

$$\mu_k^{(t+1)} = \frac{\sum_{j=1}^{N} p_{k,j}^{(t+1)} \xi_j}{E_k^{(t+1)}} \tag{11}$$

$$\Sigma_k^{(t+1)} = \frac{\sum_{j=1}^{N} p_{k,j}^{(t+1)} \left(\xi_j - \mu_k^{(t+1)}\right)\left(\xi_j - \mu_k^{(t+1)}\right)^T}{E_k^{(t+1)}} \tag{12}$$

The iteration stops when $\frac{\mathcal{L}^{(t+1)}}{\mathcal{L}^{(t)}} < C_1$, with the log-likelihood $\mathcal{L}$ defined as

$$\mathcal{L}_\Theta = \frac{1}{N} \sum_{j=1}^{N} \log\left(p\left(\xi_j\right)\right) \tag{13}$$

where C_1 is a selected threshold for convergence and t represents the current value while $t+1$ represents the estimated or new value. 3 shows a block diagram of the EM algorithm.

In this phase, a single 2D periodic motion demonstration was recorded. Using (2), (3), and (4), FSC was computed from each demonstration. Given the model and characteristics of the demonstrated behavior, polar coordinates (r, θ) for every single time step are computed. These computed values and the FSC are the inputs to the GMM. The top diagram in 4 shows a visual explanation of the demonstration phase. The obtained GMM parameters will be used by the GMR in the reproduction phase.

4.3.2. Reproduction Phase. In the reproduction phase, the previously computed Ω parameters and the GMR algorithm are used to retrieved and estimate Δ that will be used in (1). The GMR algorithm uses the Gaussian conditioning theorem and linear combination properties of Gaussian distributions to retrieve the values.[24] The GMR algorithm uses temporal values (ξ_p) as query points to estimate the corresponding values $\left(\hat{\xi}_\Delta\right)$ through regression. Given a set of values for the kth component of a GMM, the representation of mean and covariance matrix is

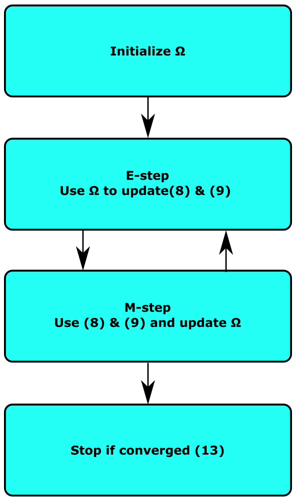

Fig. 3. Block Diagram of EM algorithm

$$\mu_k = \{\mu_{t,k}, \mu_{s,k}\}, \Sigma_k = \begin{pmatrix} \Sigma_{t,k} & \Sigma_{ts,k} \\ \Sigma_{st,k} & \Sigma_{s,k} \end{pmatrix} \tag{14}$$

The conditional expression and estimated conditional covariance of $\xi_{\Delta,k}$ given ξ_p are calculated for each GMM component k as

$$\hat{\xi}_{\Delta,k} = \mu_{\Delta,k} + \Sigma_{\Delta p,k} \left(\Sigma_{p,k}\right)^{-1} \left(\xi_p - \mu_{p,k}\right) \tag{15}$$

$$\hat{\Sigma}_{\Delta k} = \Sigma_{\Delta,k} - \Sigma_{\Delta p,k} \left(\Sigma_{p,k}\right)^{-1} \left(\Sigma_{p\Delta,k}\right) \tag{16}$$

By considering the complete GMM, the expected distribution is defined by

$$p\left(\xi_\Delta | \xi_p\right) = \sum_{k=1}^{K} \beta_k \mathcal{N}\left(\xi_{\Delta,k}; \hat{\xi}_{\Delta,k}, \widehat{\Sigma}_{\Delta,k}\right) \tag{17}$$

where

$$\beta_k = \frac{p(p|k)}{\sum_{i=1}^{K} p\left(\xi_p | i\right)} \tag{18}$$

Conditional expectation $\hat{\xi}_\Delta$ and conditional covariance $\widehat{\Sigma}_\Delta$ of the ξ_Δ given ξ_p can be approximated by a single Gaussian distribution with parameters

$$\hat{\xi}_\Delta = \sum_{k=1}^{K} \beta_k \hat{\xi}_{\Delta,k} \quad , \quad \widehat{\Sigma}_\Delta = \beta_k^2 \widehat{\Sigma}_{\Delta,k} \tag{19}$$

The GMR model only needs the means and covariance matrices of the GMM to retrieve the signal. This helps to use memory more efficiently. To compute these values, GMR needs two inputs. The first input is the GMM parameters, while the second one is a periodic position vector in polar coordinates. Given a periodic motion, the GMR can compute the estimated FSC. 4 shows a block diagram of the proposed algorithm. In this figure,x, y represent the current robots end effector position, $\tilde{x}, \tilde{y}$ represent the FS

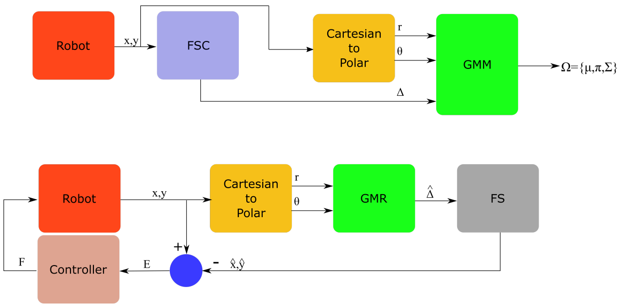

Fig. 4. Block diagrams of the system used for task three. The top figure shows a block diagram to describe the learning phase. The bottom figure shows a block diagram that describes the reproduction phase.

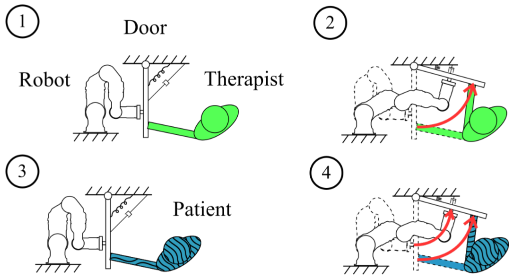

Fig. 5. Bottom Figure: Sequential training mode. During the training phase (stage 1 and 2) the therapist interacts with the robot to teach it about the task performance. Later, during the reproduction phase (stage 3 and 4), the therapist is no longer involved in the therapy. The robot helps the patient to perform the task as taught by the therapist.

estimated position, $\hat{x}, \hat{y}$ represent the GMR estimated position, E represents the error between the FS estimated position and the estimated position computed by the GMR, $\hat{\mu}$ is the mean value obtained by the GMR (estimated FSC), and F represents the force needed to move the robot to the computed estimated position. In the next section, an experiment demonstrates the power and capabilities of this new algorithms.

5. Experiments

To perform the experiment, we used a planar haptic-enabled rehabilitation robot (Quanser, Inc. Markham, Canada).[25] We used the sequential training mode to implement the learning and imitation of therapy. 5 shows the sequential training mode. In the sequential mode, first, the therapist interacts with the robot to train the system and later in the absence of the therapist and during the reproduction phase, the patient interacts with the robot. So far, we have tested the system with a non-disable user. The feasibility and efficacy of the proposed framework are evaluated by conducting the experiment simulating an adult with cerebral palsy symptoms by using transcutaneous electrical nerve stimulation and a spring array. Therefore, the word patient is used in this experiment to refer a healthy user with a simulated disability. 6 shows the reproduction phase setup.

6. Results

In this section, we present the obtained results of the experiments. The way they are presented is as follows: First, the patients task performance assisted by the robot is compared against the therapists demonstration of the task. As a numerical analysis, the correlation, as well as the mean-square error (MSE), are computed to show the similarity between the therapists performance and the patients performance.

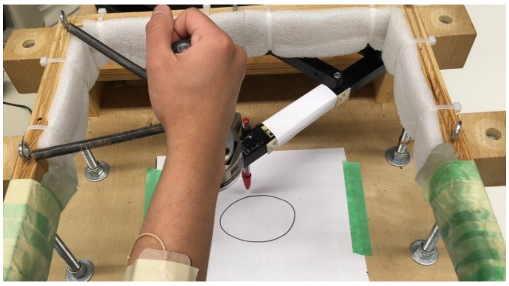

Fig. 6. Figure showing the reproduction phase. The patient interacts with the robot to execute the given task, in the therapists absence, the robot assists the patient to complete and perform the task just as the therapist did.

Table I . Numerical analysis of 1D periodic motion.

Method	Assisted-X	Non-assisted-X
CC	0.9126	0.0577
MSE	0.0002	0.0756
ED	2.2567	6.7547

6.1. First Scenario

In the first scenario, we analyze and compare the therapists behavior against the patient performance in the reproduction phase with and without robotic assistance. 7 shows the robots end effector trajectory along the X-axis, the orange and dashed line represents the therapists demonstration, the blue and solid line represents the patients reproduction with robotic assistance, while the black and solid line represents the patients performance without assisted by the robot. As can be seen, the system created a general model of the signal using the FS algorithms previously described. Based on the visual analysis, the assisted reproduction looks similar to the therapists demonstration; on the other hand, the non-assisted reproduction does not match the therapists demonstration at all. The next visual analysis runs in the frequency domain. 7 shows the power spectrum of the patients reproduction with and without robotic assistance. In this figure, the power spectrum of the therapists demonstration is shown to compare the results. As can be seen, the assisted reproduction shows better and more accurate result, while the non-assisted reproduction does not share similarities in the frequency domain. Finally, Table I shows the obtained results of the correlation coefficients (CC), mean square error (MSE), and Euclidian distance (ED) analysis. Notice that a value close to 1 in the CC means a high corralation between the reproduction and the demonstration; a small value in the MSE means small difference between the reproduction and the demonstration; finally a small value in the ED means a close similarity between the reproduction and the demonstration. The obtained results do not differ from the previous visual analysis. They help us to confirm that the patients reproduction with robotic assistance is much better than the non-assisted reproduction.

6.2. Second Scenario

The first analysis for the second scenario shows the patients reproduction with and without assistance and the therapists demonstration in X-axis and Y-axis by separate in 8. As can be seen in both figures, the assisted reproduction follows the therapists demonstration for almost 15 seconds. Due to the methodology used to learn the therapists demonstration, the system uses fix FSC that do not allow adaptability to different inputs. In other words, the system works in open loop. 8 shows the 2D patients reproduction with and without assistance and the therapists demonstration. The visual results confirm that the assisted reproduction is better than the non-assisted reproduction. Notice that due to the open loop, therefore improvement is needed to make it more real and natural. The next step in the analysis uses the power spectrum of the patients reproduction with

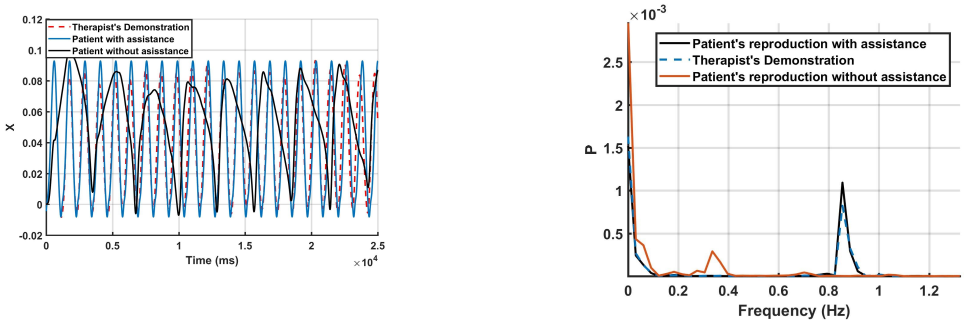

Fig. 7. Left: Therapists demonstration and patients reproduction with and without robotic assistance in X-axis. Right:Power Spectrum analysis of patients reproduction with and without robotic assistance and therapists demonstration.

Table II . Numerical analysis of 2D periodic motion.

Method	Assisted-X	Assisted-Y	Non-assisted-X	Non-assisted-Y
CC	0.7877	0.8229	0.0306	0.1259
MSE	0.0004	0.0005	0.0019	0.0028
ED	3.2729	3.6197	6.8751	8.2964

and without robotic assistance and the therapists demonstration. 8 shows the patients reproduction with and without assistance in X-axis. Notice that, because Y-axis shows a similar result it is not included. The obtained results show that the assisted and non-assisted reproduction for X-axis and Y-axis share similarities with the therapists demonstration. Both reproductions are close to the main frequency presented during the demonstration. As a general result, we can say that the assisted reproduction is slightly better than the non-assisted reproduction, but a final statement cannot be taken based on this analysis.

One more time, and as in the previous scenario, the obtained results of the CC, MSE, and ED are presented in Table II. As can be seen, some results (like MSE) present a similar conclusion for the assisted and non-assisted reproduction, while other results (like CC) give a clearer idea about the best reproduction.

6.3. Third Scenario

Finally, the obtained results of the third scenario are shown and discussed using a similar methodology as the one presented for the analysis of the previous scenarios. First, we compare the robots end effector trajectory of the therapists demonstration, against the patients reproduction with and without assistance of the robot. 9 compare the demonstration and reproductions along the X-axis and Y-axis. As can be seen in both graphs, the therapists demonstration and the patients reproduction assisted by the robot have some mismatch for a couple of seconds, also, notice that the frequency of the patients reproduction assisted by the robot has some changes during the reproduction. As mentioned before, the controller allows the patient to have freedom along the normal; for this reason, the patients reproduction assisted by the robot experimented a small mismatch. Notice that despite the mismatch between the therapists demonstration and the patients reproduction assisted by the robot during the first seconds, the system adjusted the parameters and assisted the patient to reproduce the demonstrated behavior. These adjustments are only possible due to the machine learning algorithms.

9 shows the robots end-effector motion in the 2D space. The results show that the original therapists demonstration and the patients reproduction assisted by the robot are very similar. On the other hand, the patients reproduction without assistance does not match the demonstrated behavior, and it can be taken as a fail attempt. Based on

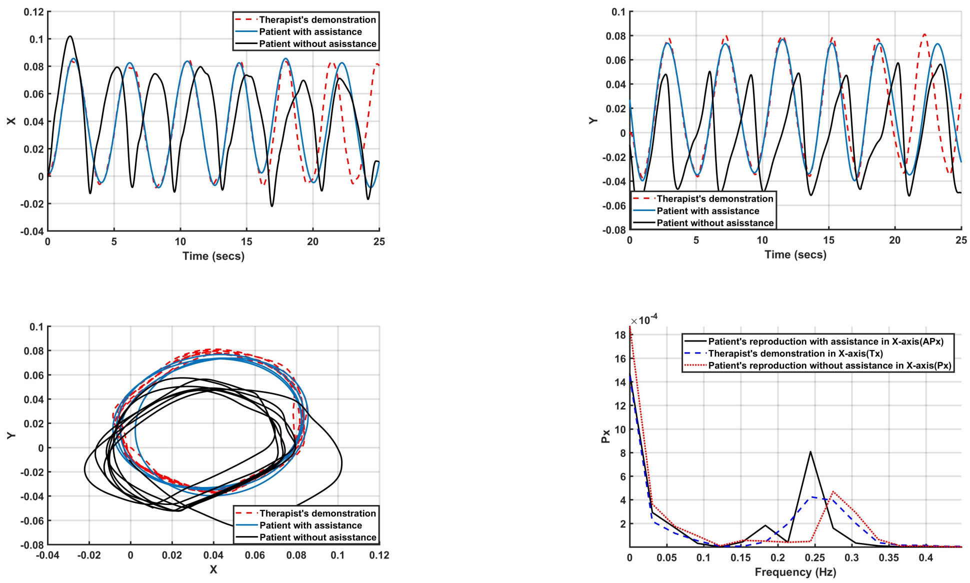

Fig. 8. Top: Therapists demonstration and patients reproduction with and without robotic assistance in X-axis (left) and Y-axis (right). Bottom: Therapists demonstration and patients reproduction with and without robotic assistance in 2D (Left) and Power Spectrum analysis of patients reproduction with and without robotic assistance and therapists demonstration in X-axis (Left).

Table III . Numerical analysis of 2D periodic motion.

Method	Assisted-X	Assisted-Y	Non-assisted-X	Non-assisted-Y
CC	0.9526	0.9541	-0.0743	-0.0539
MSE	0.0001	0.0001	0.0021	0.0035
ED	1.5112	1.7967	6.9389	8.9547

these results, we can conclude that FS + GMM-GMR algorithms can learn and reproduce the therapists behavior accurately.

Finally, 9 shows power spectrum of the patients reproduction with and without assistance in X-axis. Notice that, because Y-axis shows a similar result it is not included. By looking at the obtained results, we can easily conclude that the patients reproduction without assistance does not match the demonstrated frequency at all. For this reason, and based on this analysis, the assisted reproduction is better than the non-assisted reproduction. The assisted reproduction shows that it has almost the same frequency and amplitude as the demonstrated behavior by the therapist. CC, MSE, and ED are used to show a numerical analysis of the reproductions. These results can be found in Table III. Notice that the numerical results presented in scenario 3 are better than the results obtained in scenario 2. The reason is that the second scenario built a general and fixed model of the demonstration and it operates in an open loop. For this reason, the second scenario shows worse results. The methodology used in scenario two cannot modify its frequency nor amplitude based on the patients behavior. In other words, the second scenario does not allow any freedom to the patient while the third scenario can help the patient to adjust his/her frequency and amplitude in real time to match the demonstration.

7. Conclusion

In this paper, an LfD technique was applied to learn and imitate a semi-periodic trajectory following a task performed through a robotic rehabilitation system. The

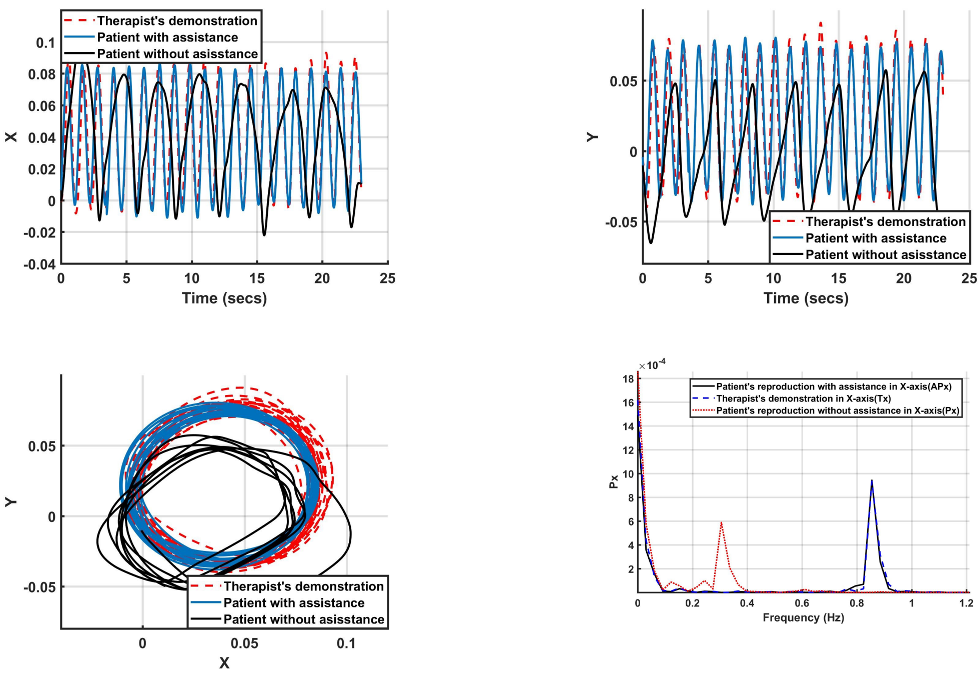

Fig. 9. Top: Therapists demonstration and patients reproduction with and without robotic assistance in X-axis (left) and Y-axis (right). Bottom: Therapists demonstration and patients reproduction with and without robotic assistance in 2D (left) and Power Spectrum analysis of patients reproduction with and without robotic assistance and therapists demonstration in X-axis (right).

demonstration and imitation phases of LfD were based upon GMM and GMR approaches, respectively. The goal was to replicate the therapists behavior accurately. In Scenarios 1 and 2, we demonstrated the effectiveness of the modeled system through an FS. The results showed an acceptable reproduction of the therapists behavior but, due to the systems nature, the results show the necessity of improvement. In Scenario 3, polar coordinates of the robots end-effector, as well as the FSC along each axis in the 2D space were recorded in the demonstration phase. A significant improvement arose due to the LfD. Thanks to the algorithms, dynamic frequencies and amplitudes of the FS are possible to be reproduced. As seen in the results, better and more accurate reproduction is possible.

References

1. World Heart Federation, "Stroke - World Heart Federation," **In**: *http://www.world-heartfederation.org/cardiovascular-health/stroke/* (2017).
2. Foundation, "Statistics - heart and stroke foundation of Canada," **In**: *heartandstroke.ca: http://www.heartandstroke.com/site/c.ikIQLcMWJtE/b.3483991/k. 34A8/Statistics.htm* (2017).
3. Assosiation, "Explaining a Stroke," **In**: *http://www.stroke.org/sites/default/files/resources/ExplainingStrokeBrochure.pdf* (2017).
4. Veerbeek et al, "Early Prediction of Outcome of Activities of Daily Living After Stroke: A Systematic Review," **In**: *Stroke* (2011) pp. 1482–1488.
5. P. Lum et al, "Robotic Devices for Movement Therapy After Stroke: Current Status and Challenges to Clinical Acceptance," **In**: *Topics in Stroke Rehabilitation* (2002) pp. 40–53.
6. N. Hogan et al, "MIT-MANUS: a workstation for manual therapy and training. I," **In**: *Proceedings IEEE International Workshop on Robot and Human Communication* (1992) pp. 161–165.
7. M. Maaref et al, "A Bicycle Cranking Model for Assist-as-Needed Robotic Rehabilitation Therapy Using Learning From Demonstration," **In**: *IEEE Robotics and Automation Letters* (2016) pp. 653–660.
8. M. Sharifi et al, "Cooperative modalities in robotic telerehabilitation using nonlinear bilateral impedance control," **In**: *IEEE Robotics and Automation Letters* (2017) pp. 52–63.

9. F. Atashzar et al, “Networked teleoperation with non-passive environment: Application to telerehabilitation,” **In**: *IEEE/RSJ International Conference on Intelligent Robots and Systems, Vilamoura* (2012) pp. 5125–5130.
10. F. Atashzar et al, “A Computational-Model-Based Study of Supervised Haptics-Enabled Therapist-in-the-Loop Training for Upper-Limb Poststroke Robotic Rehabilitation,” **In**: *IEEE/ASME Transactions on Mechatronics,* (2018) pp. 563–574.
11. L. Legg et al, “Occupational therapy for patients with problems in activities of daily living after stroke,” **In**: *Cochrane Stroke Group,* (2018).
12. J. Fong and M. Tavakoli, “Kinesthetic Teaching of a Therapist’s Behavior to a Rehabilitation Robot,” **In**: *International Symposium on Medical Robotics (ISMR),* (2018).
13. H. Lee et al, “Learning basis skills by autonomous segmentation of humanoid motion trajectories,” **In**: *IEEE-RAS International Conference on Humanoid Robots,* (2012) pp. 112–119.
14. M. Guidali et al, “A robotic system to train activities of daily living in a virtual environment,” **In**: *Medical and biological engineering and computing,* (2011) pp. 1213–2011.
15. S. Calinon et al, “On learning the statistical representation of a task and generalizing it to various contexts,” **In**: *IEEE International Conference on Robotics and Automation,* (2006) pp. 2978–2983.
16. E. Gribovskaya et al, “Learning nonlinear multi-variate motion dynamics for real-time position and orientation control of robotic manipulators,” **In**: *Humanoid Robots,* (2009) pp. 472–477.
17. G. Konidaris et al, “Robot learning from demonstration by constructing skill trees,” **In**: *The International Journal of Robotics Research,* (2012) pp. 360–375.
18. R. Tao, “Haptic Teleoperation Based Rehabilitation Systems for Task-Oriented Therapy,” **In**: *M.S. thesis, Dept. Electrical and Computer Eng., University of Alberta, Alberta, Canada, 2014* (2014).
19. C. Martinez, J. Fong, and M. Tavakoli, “Learning and Imitation of a Therapists Interaction with a Patient in Robot-assisted Cooperative Therapy Exercises,” **In**: *Unpublished,* (2018).
20. K. Kido, “Digital Fourier analysis: fundamentals,” **In**: *TUndergraduate Lecture Notes in Physics,* (2015).
21. S. Calinon and A. Billard, “Incremental learning of gestures by imitation in a humanoid robot,” **In**: *ACM/IEEE International Conference on Human-Robot Interaction,* (2007) pp. 255–262.
22. S. Calinon, “A tutorial on task-parameterized movement learning and retrieval,” **In**: *Intelligent Service Robotics,* (2016) pp. 1–29.
23. S. Calinon et al, “Statistical dynamical systems for skills acquisition in humanoids,” **In**: *IEEE-RAS International Conference on Humanoid Robots,* (2012) pp. 323–329.
24. S. Calinon, “Robot programming by demonstration,” **In**: *EPFL Press,* (2009).
25. C. Lu et al, “Development of a robotic device for upper limb stroke rehabilitation: A user-centered design approach,” **In**: *Paladyn,* (2011) pp. 176–184.